Coastal Dynamics 2017
Paper No. 120

SEDIMENT MOVEMENT INDUCED BY SHIP-GENERATED WAVES IN RESTRICTED WATERWAYS

Magnus Larson[1], Björn Almström[1], Gunnel Göransson[2], Hans Hanson[1], and Per Danielsson[2]

Abstract

This study focuses on the sediment transport by ship-generated waves in restricted waterways. Two data sets from Göta River in Sweden, an important shipping lane on the Swedish west coast, were analyzed in detail to determine the impact of ship waves, namely (1) continuous recordings of turbidity at seven stations along the river with 1-min resolution; and (2) dedicated field campaigns to measure water level and turbidity during ship passages. Measured turbidity was related to the suspended sediment concentration (SSC) and used as a proxy for the sediment transport. Several existing formulas were tested to evaluate their capability to predict both the primary and secondary waves, and the PIANC formula yielded the overall best agreement for the secondary (divergent) waves and a relationship based on the vessel sinkage for the primary (drawdown) waves. The turbidity (SSC) was found to depend primarily on the drawdown wave properties and empirical equations were derived to estimate the maximum turbidity during a ship passage at the study site. Finally, the advection-diffusion equation was used to model the impact of the ship on the sediment transport by describing it as moving source. The fit of an analytical solution to turbidity measurements indicated the potential for this type of rather simple model.

Key words: sediment transport, ship waves, bed and bank erosion, advection-diffusion equation, turbidity, suspended sediment concentration

1. Introduction

Ships traveling in restricted waterways induce water motion that can move sediment, which in turn causes erosion of the bed and the banks (the shore). The most visible types of such motion are the surface waves that are generated when the ship pushes away water as it moves forward. Two main types of waves originate from a ship, namely primary (drawdown) and secondary waves (Havelock, 1908; Bertram, 2000), where the former is associated with the displacement of the water because of the hull and the latter with the disturbances at the bow and the stern (divergent and transverse waves, respectively; Sorensen, 1967, 1997). The primary wave becomes increasingly important in restricted waterways, where the ship may block a significant portion of the cross-sectional area. Regarding the secondary waves, the transverse waves decay faster than the divergent waves and typically have smaller heights, implying that in general only the divergent waves potentially cause significant sediment movement near the shore. The drawdown has a much longer period than the divergent waves, leading to larger velocities and sediment transport in shallow water. Also, the drawdown tends to arrive first at the shore, initially causing a marked decrease in water level, followed by a package of 5-10 waves representing the divergent waves.

Worldwide, problems related to sediment transport and erosion due to ship waves have increased during the latest decade because of more traffic and larger ships traveling at higher speeds. Although the ship hulls have designs to reduce the secondary waves, the primary waves are difficult to eliminate and often cause the major impact on the bed and banks in restricted waterways. The main objective of the present study was to investigate ship-generated waves and their effects on sediment transport and erosion in restricted waterways. Two field sites in Sweden were subject to investigation, namely Göta River (GR) on the Swedish west coast and Furusundsleden (FL) in the Stockholm Archipelago, both being important shipping lanes with erosion

[1]Department of of Water Resources Engineering, Lund University, Box 118, 22100 Lund, Sweden.
magnus.larson@tvrl.lth.se; bjorn.almstrom@tvrl.lth.se; hans.hanson@tvrl.lth.se
[2]Swedish Geotechnical Institute, Hugo Grauers Gata 5B, 41296 Göteborg, Sweden.
gunnel.goransson@swedgeo.se; per.danielsson@swedgeo.se

problems related to ship waves. Data collection at the sites included water level variation and turbidity (a proxy for sediment movement; (compare with Ravens and Thomas, 2008; Rapaglia *et al.*, 2010; and Gelinas *et al*., 2013)) near the shore together with mapping of bank erosion. In the next phase of the work, nature-based erosion protection will be studied through full-scale testing in FL.

The focus of the present paper is on the measurements and modeling carried out in GR, since the study in FL is still in its initial phase. First, a brief introduction to ship-generated waves is provided together with their possible effects on river beds and banks, followed by a description of the study site in GR. The field measurements are then reviewed and some basic properties of the collected data are discussed. Different types of models are employed to reproduce the observed data, both regarding the wave properties and the sediment transport. As a proxy for the latter, the suspended sediment concentration is used derived from detailed measurements of the turbidity. The models employed include both empirically derived relationships and more physics-based formulations, for example the advection-diffusion equation (ADE). The paper ends with a set of conclusions and an outlook regarding future work to be performed, mainly in FL.

2. Ship-Generated Waves

Although several different types of water motion is induced by ships traveling in a restricted waterway, for example, propeller jets and increased velocity due to the reduction in flow cross-sectional area, the focus here is on the generated surface waves and their effects on the bed and the banks of the waterway. In the following a brief discussion is given on the hydrodynamics, sediment transport, and morphological change that are associated with such waves.

2.1. *Hydrodynamics*

The primary wave (drawdown) is a result of the pressure and velocity distribution along the moving ship hull, having a wavelength of the same order as the length of the ship. The secondary waves, the divergent and transverse waves, are generated by the disturbances at the bow and the stern, respectively, where the names refer to the propagation direction of the wave. In deep water, the divergent waves propagate away from the sailing line of the ship at a theoretical angle of 35.3 deg. The drawdown is typically negligible in the open sea; however, in restricted waterways it is often the most important wave component in terms of size and impact on bed and banks. Figure 1 illustrates the passage of a ship at one of the measurement stations in GR and the generated primary wave at the shore. In the figure a poorly constructed rubble-mound revetment for erosion protection may also be seen along the river bank.

(a) (b)

Figure 1. (a) The ship Patria approaching the measurement station (Garn); (b) the resulting primary wave (photos by Jonas Althage).

The properties of the ship-generated waves (both primary and secondary) depend on many factors, related both to the characteristics of the ship and the waterway (Kriebel and Seelig, 2005). The main factors associated with the ship are the dimensions (length and width), hull design, draft, and velocity, whereas the ones related to the waterway are flow velocity, clearance depth, cross-sectional area, and shape. The distance

from the sailing line is also of importance, especially for the secondary wave height which decays with distance from the ship. In general, the ship velocity relative to the flow velocity is the most important factor, especially for the secondary waves, where a larger relative velocity yields higher waves and longer periods. The volume displaced by the ship, which is a function of the length, width, and draft, determines the drawdown height and wavelength, where a larger volume implies a larger height and a longer period. Also, the larger the area is that the ship occupies with respect to the cross-sectional area of the waterway, the higher the drawdown will be.

Figure 2 displays the typical features of a wave train generated by a ship in a restricted waterway, including both the primary and secondary waves (measurements performed in FL, close to shore; for more details see Granath, 2015). Since the drawdown has a much longer wavelength than the secondary waves, the speed will be higher and the drawdown wave will arrive first with a marked trough; subsequently a wave package containing the divergent waves may be observed involving 10-15 individual waves. The effects of the drawdown appears again after the divergent waves have decayed, probably because of some standing wave motion induced by the local bathymetry. Possibly some effects of the transverse waves, superimposed upon this standing wave may be identified, although their influence is small. With regard to their wavelengths, the drawdown waves may be treated as shallow-water waves, whereas the secondary waves are deep-water waves.

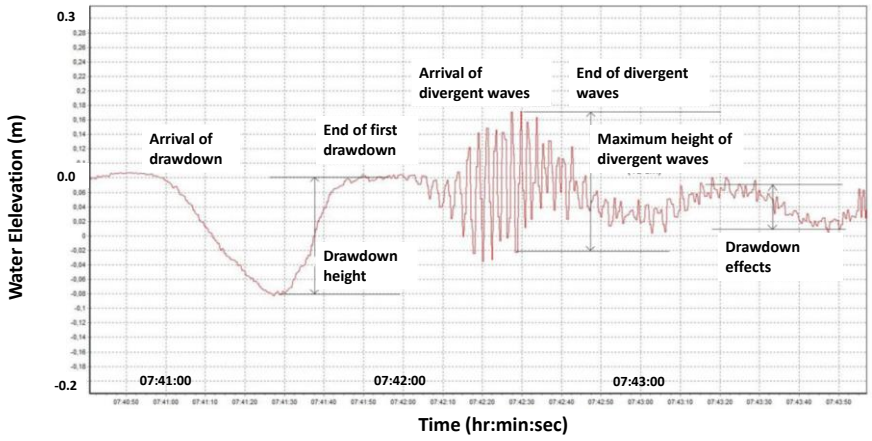

Figure 2. Example of a train of primary (drawdown) and secondary (divergent and transverse) waves generated by a ferry in Furusundsleden (after Granath, 2015).

2.2. *Sediment transport and morphological change*

Ship waves may mobilize and transport sediment, especially in the nearshore areas where both the bed and the banks are exposed to wave-generated flows. Typically, in restricted waterways are the conditions sheltered towards wind-generated waves, implying that the ship waves can be the main cause of sediment transport and erosion, although they are not occurring that frequently (on an open coast the wind waves are almost always dominant and the contribution from ship waves are negligible). Also, in waterways the sediment is often fine, which means that less bed shear stress is required for initiation of motion and transport; thus, ship waves may be sufficiently large to transport material. In addition, steep banks of easily eroded material are often present along waterways that will suffer from wave impact. As an example, Figure 3 shows an eroding bank that is suffering from ship wave impact in FL, a major shipping lane in the Stockholm Archipelago where large ferries and cruise ships regularly travel. In this archipelago, the banks consists of moraine deposited during the latest ice age that includes a wide range of grain sizes.

On the bed, it is the shear stress due to the oscillatory motion that may induce transport. If a flow is present in the waterway, as is the case for a river, the sediment mobilized by the waves can be transported by the mean currents due to this flow; thus, it is often the combination between the waves and the currents that transports the sediment. The shear stress due to the waves is typically much larger than the stress from the mean currents because of the thinner boundary layer; however, the waves typically induce negligible mean currents that cause transport. If the waves hit a steep bank, it is the impact force that will generate transport

and erosion. In the case of bank erosion there is no possibility of recovery (*i.e*., accretion), which may occur on an eroded stretch of the bed depending on the material and the transport gradients. However, if coarser material is present in the banks, a cobble beach may develop that protects the bank, although this may take long time and require a significant shoreward translation of the bank, all depending on the availability of coarse material in the bank.

(a) (b) (c)

Figure 3. (a) A large ferry passing close to shore in Furusundsleden; (b) the long-term effects on the banks due to the impact from both primary and secondary waves; (c) a cobble beach that developed after wash-out of fine material due to wave impact (photos by Magnus Larson).

3. Study Site Göta River (GR)

3.1. *Field measurements*

The field measurements discussed here were performed in the downstream stretch of the Göta River (GR), which is the largest river by flow in Sweden (for location of the river, see Figure 4). This stretch runs from Lake Vänern to the city of Gothenburg, where the river discharges its water to the sea through two branches. The lower part of GR is a major waterway for shipping and about 1,600 ships travel here annually. The size of the ships are determined by the dimensions of the locks present in the river, implying a length of around 80 m and a width of 12 m with a draft in the range 3-5 m. In GR the maximum speed for the ships is 10 knots, but along some sensitive parts of the river this speed is lowered to 5 or 7 knots. The measured mean flow in the river is 516 m^3/s and the maximum recorded flow 1,033 m^3/s. A typical cross section of the river is 6-9 m deep and 150-200 m wide (Göransson *et al*., 2012). The material in the river bed and banks is mostly fine, classified as clayey silt or silty clay.

Two types of data were employed in the present study to analyze ship waves and their impact on the sediment transport. The first data set originates from continuous recordings of turbidity carried out by the City of Gothenburg at seven stations along the GR as one-minute averages. The turbidity values discussed here were measured in FNU, which is recommended in the Swedish standard. Calibration based on water samples showed that 1 FNU corresponds to 1 mg/l of suspended sediment concentration (SSC) for the study site (Althage, 2010). A period during the summer of 2006 was selected for the analysis of the impact of ship waves on the sediment transport using the turbidity as a proxy. The second data set was obtained through dedicated field experiments in connection with ship passages, where in total 17 passages were observed at Station Garn (see Figure 4) during which the detailed water and turbidity variation in time were measured. The water level was recorded with a video camera and subsequently digitized, which allowed for an evaluation of primary and secondary waves. The measurement station was located about one ship length from the sailing line of the ship.

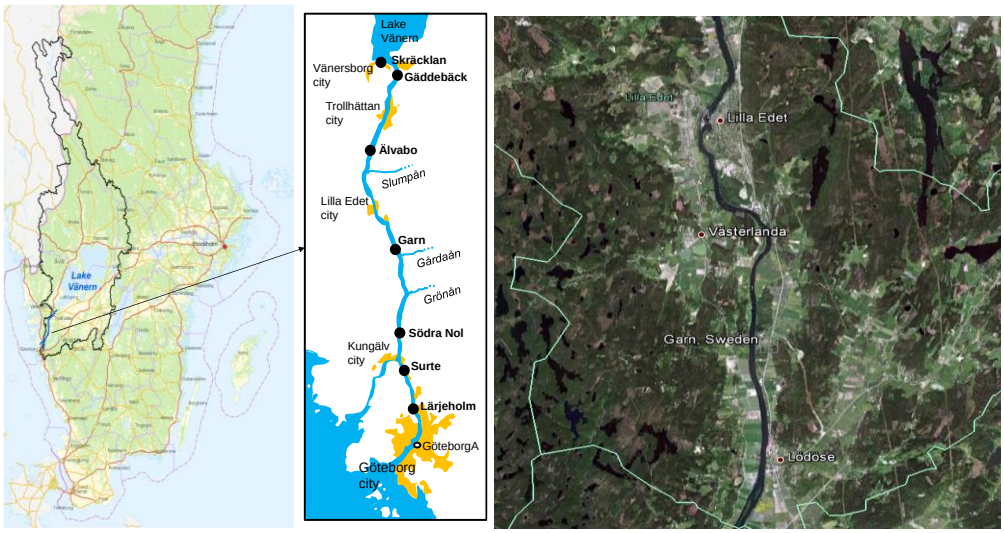

(a) (b) (c)

Figure 4. (a) Location of study site for ship waves in Göta River; (b) the measurement stations for turbidity recordings (after Göransson, 2014); (c) details of the river around the measurement station Garn.

3.2. *Data collected and their properties*

As a typical example, Figure 5a illustrates the recorded turbidity during a number of ship passages at Station Garn; a steep increase in turbidity is observed up to a maximum level, followed by a gradual decay back to a base level corresponding to the background concentration in the river. In order to determine the properties of the turbidity events induced by ship passages, 101 such events were identified during the summer of 2006 from the continuous turbidity measurements. Station Garn was employed in this analysis since the signal due ship passages typically are very clear at this station (the river is rather straight over a considerable distance and the flow conditions simple), although similar turbidity responses could be observed at the other stations as well. Also, only events that produced a maximum turbidity that exceeded twice the base level was selected to obtain events with a marked response. The ship responsible for a specific turbidity event was not identified; thus, no correlation between ship properties and induced turbidity events could be made for the continuously recorded series.

A number of parameters were determined for a specific turbidity event, including maximum (peak) and mean turbidity, duration of event, time to peak from start of event, total area under the turbidity curve (related to the total mass transport during the event), and decay rate after the peak (by fitting an exponential function). The base level of the turbidity before the event was estimated and subtracted from the values recorded during the event before further analysis. The mean of the base level turbidity for all events was 5.2 FNU (or mg/l of SSC) with a standard deviation of 0.98 FNU. For the peak turbidity, a mean value of 12 FNU was obtained (above base level) and the maximum value recorded was 39.6 FNU. Different definitions of the event duration were employed, including based on visual inspection (somewhat subjective) and fitting an exponential decay (end of event defined to occur at a certain turbidity level). These definitions did not result in significantly different estimates, but the mean event duration was about 40 min with a variation from 15 to 140 min. Since the passage of a ship generates wave motion at the site that typically lasts only 1-2 min, which approximately corresponds to the time to the peak, advection, dispersion, and settling affect the material mobilized by the waves to produce the observed time variation in turbidity that lasts much longer than the ship passage.

Figure 5b shows the 101 events plotted by normalizing the turbidity during each event with the peak value and the time with the event duration. Although the scatter is significant, the shape of the turbidity response is similar for the events with a fast rise towards the peak, which typically occurs within the first 10% of the event duration, followed by an approximately exponential decay back to the base level. In a few cases a smaller peak appeared before the major peak, causing the latter to occur later during the event that explains some of the scatter in the data plotted. Fitting an exponential function to the decaying part of the

event yielded a spatial decay coefficient of about 0.12 min^{-1}.

The data collected on water level and turbidity during individual ship passages included 17 events where the ship dimensions, shape, draft, and speed were also recorded as well as the river flow, velocity, and water depth (Göransson *et al*., 2014). These data were primarily employed to test different equations for predicting the wave height and period (primary and secondary waves) together with the turbidity induced during ship passage. Both the measured drawdown and divergent wave height varied approximately between 0.1 and 0.6 m for the studied events. The drawdown period was in the range 20 to 60 s, whereas the half-period of the divergent wave varied from 0.5 to 1.5 s. The maximum turbidity observed during the events was 17 FNU and the minimum 0 FNU (no sediment mobilization).

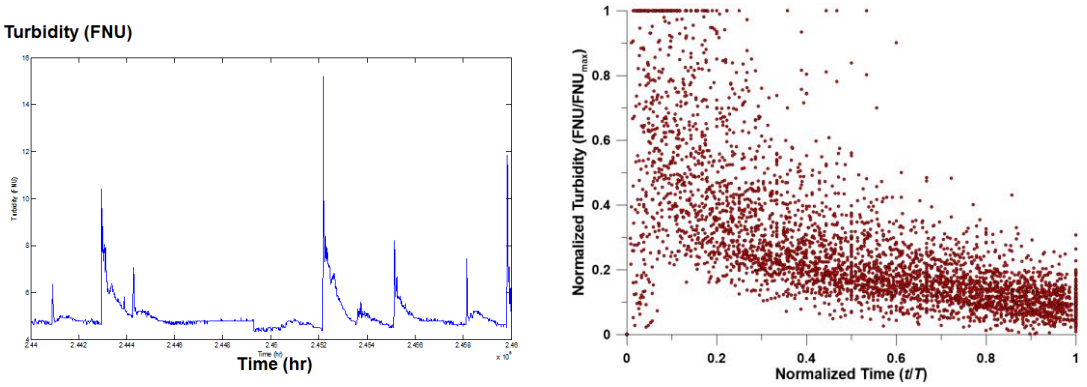

(a) (b)

Figure 5. (a) Example of measured turbidity at Station Garn during several ship passages; (b) variation in turbidity with time elapsed during 101 ship passages using maximum turbidity and event duration as normalizing quantities.

4. Modeling of Ship Waves

4.1 *Models of ship waves*

A number of predictive formulas have been proposed for ship waves, especially for the secondary waves (*i.e.*, divergent waves). Typically, such formulas are expressed in non-dimensional form containing a Froude number based on the water depth or ship length (see Kriebel and Seelig, 2005). The former number would be most relevant in shallow water and the latter in deeper water; however, some formulas include a more general Froude number that weighs the effects of both shallow and deep water (Kriebel *et al*., 2003). Examples of formulas to predict the secondary waves have been proposed by Sorensen and Weggel (1984), PIANC (1987), Sorensen (1997), and Kriebel and Seelig (2005) and for the primary waves by Kriebel *et al*. (2003) and USACE (2006), although the latter reference refers to the vessel sinkage which is closely related to the drawdown. The speed (C) of the divergent waves coming of the ship is $C = V_{SR}\cos\theta$, where V_{SR} is the ship speed relative the water and θ the wave angle (theoretically 35.3 deg in deep water). Assuming that deep water prevails for the divergent waves, the wave period (T_W) will then be $T_W = 2\pi V_{SR}\cos\theta / g$.

4.2 *Model comparison with data*

Comparison between the measured divergent waves and different predictive formulas showed that the one proposed by PIANC (1987) yielded the best results (compare Atzeni and Sulis, 2012); however, the scatter was significant and the normalized root-mean-square error was ε = 0.40. No attempt was made to modify the coefficients in the formula, but the recommended values were employed. Figure 6a summarizes the analysis results, where the predicted maximum wave height from the PIANC formula was plotted against the measured maximum wave height for each ship passage (the straight line denotes perfect agreement). The other formulas that were investigated with less good agreement were Sorensen (1997) and Kriebel and Seelig (2005). Spectral analysis was performed for each group of divergent waves and the peak period obtained was compared with predictions by the theoretical expression previously given (assuming deep water conditions)

and good agreement was found. A linear regression between the half-period, often used in the study of ship waves, and the peak spectral period yielded a slope of the line somewhat less than the expected 0.5 (Göransson *et al.*, 2014).

To predict the maximum drawdown wave height, the formula by Kriebel *et al.* (2003) was used and comparted with the measured heights; however, the scatter was pronounced, especially for some of the larger waves. Instead the correlation between the drawdown and the vessel sinkage was investigated and an improved relationship was developed based on regression analysis (see Figure 6b). Initially a linear fit was employed, but using a nonlinear fit improved the agreement with ε = 0.39. Purely empirical formulas were also tested where different non-dimensional groups involving the main ship and river parameters were included, but the agreement obtained did not improve markedly. One such formulas expressed the maximum drawdown wave height normalized with the draft as a function of a depth-based Froude number and the ship width divided by the clearance depth.

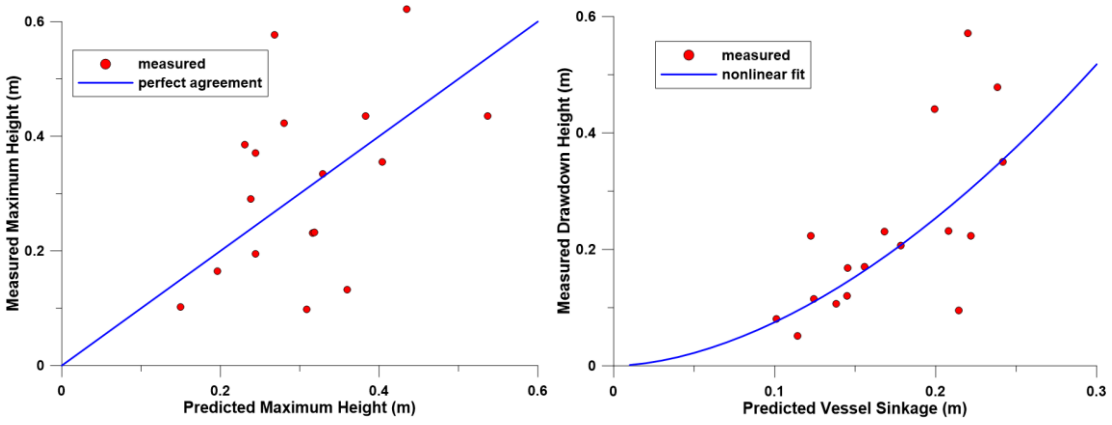

(a) (b)

Figure 6. (a) Predicted maximum divergent wave height from formula by PIANC (1987) compared with measured wave height; (b) Measured drawdown plotted against predicted vessel sinkage from formula by USACE (2006) (after Göransson *et al.*, 2014).

5. Modeling of Sediment Transport

5.1 *Models of sediment transport*

No simple formulas are available to predict the turbidity (or SSC) in a river due to ship passages. In this study, two approaches were taken: (1) empirical models based on regression analysis involving non-dimensional quantities or a simple description of the physical processes; and (2) the advection-diffusion equation (ADE) to describe the mobilization and transport, including advection, diffusion (or, more correctly, dispersion), and sedimentation. The former approach focused on the data from the dedicated measurements, whereas the latter employed data from the continuous recordings. In the application of the ADE, simplifications were introduced to allow for analytical solutions and the comparison with data focused on the overall properties of the ship-induced turbidity.

In order to model the turbidity (or SSC) with the ADE due to the passage of a ship mobilizing sediment, the simplest approach is to assume that the ship may be described as a moving source. Once the sediment has been brought up from the bed it will be subject to transport and mixing by advection, dispersion, and settling. For the one-dimensional case, assuming constant mean velocity, water depth, dispersion coefficient, and settling velocity in the river, the ADE may be written,

$$\frac{\partial c}{\partial t} + U\frac{\partial c}{\partial x} = D\frac{\partial^2 c}{\partial x^2} - \frac{wc}{h} \qquad (1)$$

where c is the concentration (SSC or, equivalently, the turbidity), U the mean velocity in the river, D the dispersion coefficient, w the settling velocity, and h the water depth. This equation describes how sediment is transported downstream with the mean velocity, at the same time being subject to dispersion and settling at the bottom (the last term on the right-hand-side acts as a sink for sediment). The solution to the above equation for the case of a release of a mass M (kg) instantaneously at $x = x_s$ and $t = 0$ is (Crank, 1975),

$$c(x,t) = \frac{M}{A\sqrt{4\pi Dt}} \exp\left(-\frac{\left(x - x_s - Ut\right)^2}{4Dt} - \frac{wt}{h} \right) \tag{2}$$

where A is the cross-sectional area of the river.

A moving source that continuously mobilizes material from the bed may be simulated through the instantaneous release of material from all the locations the moving source passed after a particular time (Eq. 1 describes the transport and mixing of material for this situation as well). The net effect of the release of the material will be obtained by superimposing analytical solutions following Eq. 2, where the complete solution at a certain time t depends on the time history of the release of material by the moving source prior to t. Thus, the effect of the material that was released at time t' is (compare Carslaw and Jaeger, 1959),

$$c(x,t) = \frac{m dt'}{A\sqrt{4\pi D\left(t - t'\right)}} \exp\left(-\frac{\left(x - x_s - Ct' - U\left(t - t'\right)\right)^2}{4D\left(t - t'\right)} - \frac{w\left(t - t'\right)}{h} \right) \tag{3}$$

where m is the amount released per unit time, dt' the duration of the release of material when the source is at $x = x_s + Ct'$ (C is taken positive when the source is moving downstream in the direction of the positive x-axis). Superimposing an infinite number of sources described by Eq. 3, implying that $dt' \to 0$, yields the following solution:

$$c(x,t) = \frac{m}{A\sqrt{4\pi D}} \int_0^t \frac{\exp\left(-\frac{\left(x - x_s - Ct' - U\left(t - t'\right)\right)^2}{4D\left(t - t'\right)} - \frac{w\left(t - t'\right)}{h} \right)}{\sqrt{t - t'}} dt' \tag{4}$$

Doing a variable transformation in Eq. 4 by introducing $\xi = \sqrt{t - t'}$ yields after some calculation:

$$\begin{aligned} c(x,t) = {} & \frac{m}{A\sqrt{\pi D}} \exp\left(-\frac{\left(C - U\right)\left(x - x_s - Ct\right)}{2D} \right) \cdot \\ & \int_0^{\sqrt{t}} \exp\left(-\left(\frac{\left(C - U\right)^2}{4D} + \frac{w}{h} \right) \xi^2 - \frac{\left(x - x_s - Ct\right)^2}{4D\xi^2} \right) d\xi \end{aligned} \tag{5}$$

The integral in Eq. 5 may be expressed in terms of elementary functions. Abramowitz and Stegun (1972) presented the following relationship,

$$\int \exp\left(-a^2 x^2 - \frac{b^2}{x^2} \right) dx = \frac{\sqrt{\pi}}{4a} \left(\exp\ 2ab\ \operatorname{erf}\left(\mathrm{ax} + \frac{\mathrm{b}}{\mathrm{x}} \right) + \exp\ -2ab\ \operatorname{erf}\left(\mathrm{ax} - \frac{\mathrm{b}}{\mathrm{x}} \right) \right) \tag{6}$$

where $a \neq 0$ and erf denotes the error function. Comparing Eqs. 5 and 6 gives the following values for the constants a and b:

$$a^2 = \frac{C-U^{\ 2}}{4D} + \frac{w}{h}$$
$$b^2 = \frac{Ct - \ x - x_s^{\ 2}}{4D} \tag{7}$$

Thus, using Eq. 6 and the definitions in Eq. 7, Eq. 5 may be expressed as:

$$c(x,t) = \frac{1}{4a}\frac{m}{A\sqrt{D}}\exp\left(-\frac{(C-U)(x-x_s-Ct)}{2D}\right)\cdot$$
$$\left(\exp(2ab)\,\mathrm{erf}\left(a\sqrt{t}+\frac{b}{\sqrt{t}}\right)+\exp(-2ab)\,\mathrm{erf}\left(a\sqrt{t}-\frac{b}{\sqrt{t}}\right)-2\sinh(2ab)\right) \tag{8}$$

In order to better display the solution given by Eq. 8 and its basic properties, the equation may be put in non-dimensional form by introducing the following variables,

$$x' = x/L, \quad x_s' = x_s/L, \quad t' = 4Dt/L^2$$
$$h' = h/L, \quad U' = UL/4D, \quad C' = CL/4D \tag{9}$$
$$w' = wL/4D, \quad c' = cDL/m$$

where L is an appropriate length scale of the problem. With these definitions the non-dimensional forms of the constants a and b will become:

$$a'^{\,2} = C'-U'^{\,2} + \frac{w'}{h'}$$
$$b'^{\,2} = C't' - \ x' - x_s'^{\ 2} \tag{10}$$

Eq. 8 can be written in the following non-dimensional form:

$$c'(x',t') = \frac{1}{8}\exp\left(-2(C'-U')(x'-x_s'-C't')\right)\cdot$$
$$\left(\exp(2a'b')\,\mathrm{erf}\left(a'\sqrt{t'}+\frac{b'}{\sqrt{t'}}\right)+\exp(-2a'b')\,\mathrm{erf}\left(a'\sqrt{t'}-\frac{b'}{\sqrt{t'}}\right)-2\sinh(2a'b')\right) \tag{11}$$

5.2 *Model comparison with data*

For the individual ship passages, the maximum turbidity correlated markedly ($r > 0.5$) with the maximum drawdown wave height, the drawdown period, the ship width, and ship shape (describe through the entrance length; see Kriebel and Seelig, 2005). Thus, at the measurement location the drawdown was more important for the turbidity than the secondary waves (compare Schoellhamer, 1996), implying that the effort to derive empirical relationships for the maximum turbidity involved primarily the drawdown and ship properties. However, since the drawdown reflects the ship properties, the regression analysis performed included mainly the drawdown properties. A reasonably small error between calculated and measured values was obtained when the maximum turbidity was related to the maximum drawdown normalized with the clearance depth.

By employing a simple model based on the estimated bed shear stress(τ_D) this error could be made significantly lower, though. The mobilization of material at the bed should be related to the shear stress, which for the drawdown might be estimated as $\tau_D = 0.5\rho f_w u_D^2$, where ρ is the water density, f_w the wave friction factor, and u_D the horizontal velocity at the bed due to the drawdown. Using shallow water wave

theory for u_D it can be shown that $\tau_D \sim s_D^2 / h$, where h is the water depth. The measured and calculated maximum turbidity is plotted in Figure 7, where an empirical equation was derived based on regression against this ratio. It should be pointed out that the coefficient obtained in this regression equation is highly site-specific and it is only the general form of the equation that may have some validity.

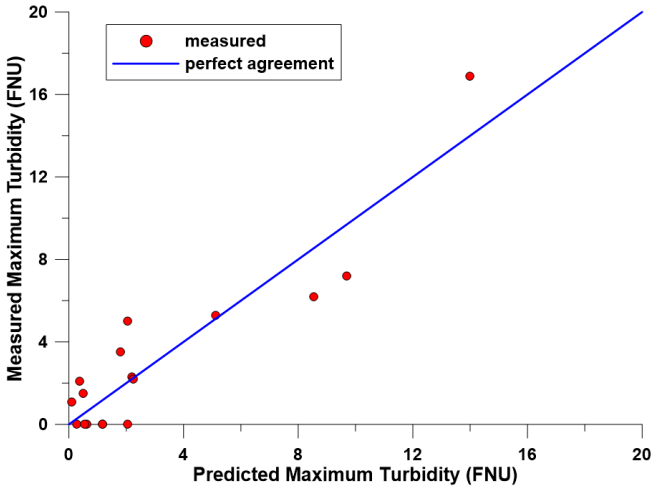

Figure 7. Comparison between measured and predicted maximum turbidity at Garn Station using a semi-empirical relationship (after Göransson *et al.*, 2014).

The solution to the ADE (Eq, 8) describing the impact of a ship on the sediment transport as a moving source was compared with the continuously collected data at Garn Station previously shown in Figure 5b. Several different parameters determine the solution, including the mobilization of the sediment at the bed by the ship (m; source strength), the ship speed (C) and direction (upstream of downstream), the advective velocity (U), the dispersion coefficient (D), and the settling velocity (w). In order to validate the overall applicability of the derived solution to describe the observed turbidity variations, the non-dimensional form of the solution (Eq. 11) was compared to the measured turbidity as a function of time, expressed in non-dimensional form, for the aforementioned discussed 101 events. The scatter in the normalized data is large in itself; thus, if each event was separately analyzed improved fits could be obtained compared to the present approach, where the parameters selected were only representative in a general sense. However, in the former approach involving the fitting of the solution to individual events, lack of information on some basic parameters would limit the value of the results, besides demonstrating that the solution could describe the observations well during an event.

Figures 8a and 8b illustrates the typical results of applying the solution given by Eq. 8 to the recorded events. The employed solution did not include initial transients related to the start of the ship, but sufficient time had elapsed for a quasi-steady distribution for develop. The main parameters were selected based on average conditions in the river during ship passage, that is, $U = 0.5$ m/s and $C = 5$ m/s (up- or downstream). The settling velocity was difficult to assess and its influence was investigated more or less through sensitivity analysis. Through the normalization, the maximum concentration does not enter into the problem as well as the event duration. In a real applications, working with dimensional quantities, these two parameters would be closely related to the ship properties and the generated wave characteristics. The length scale (L) introduced is arbitrary, but is included in all non-dimensional quantities and will scale the solution (see Eq. 9). A difficult parameter to estimate is the dispersion coefficient (D); previous studies in GR have employed values in the range 100-200 m^2/s based on existing empirical formulas (Göransson *et al.*, 2012). For convenience, it was assumed here that the length scale was set to a value similar to the dispersion coefficient, implying that they would cancel out in the main non-dimensional quantities involved in the solution presented here. Again, employing the dimensional solution for obtaining quantitative predictions will require that a lot of the parameters are assigned appropriate values.

In Figure 8a is the solution given for a ship traveling upstream or downstream using the previously mentioned parameter values together with the measurements. A non-dimensional value on the settling

velocity was set to $w' = 0.5$, which implied a w that is significantly larger than the value reported by Göransson *et al*. (2012). However, because the advective speed is relatively small, marked sedimentation is needed to achieve the proper decay in turbidity (SSC) that is observed after the passage of the ship. If the ship is traveling downstream (in the direction of the flow), the decay is somewhat larger and in better agreement with a majority of the data. It should be pointed out that the direction of travel for the ships during the recorded 101 events is not known. Figure 8b shows the same solution but where the ship is traveling upstream for two different normalized settling velocities ($w' = 0.5$ and 1.0). For the parameter values employed, increasing the settling velocity produces a better fit, at least during the most of the period during which the turbidity is decreasing after the peak. Overall, the comparisons between the schematic applications of the derived solution and the recorded turbidity events indicate a potential for the solution to be used in describing the sediment transport induced by ships in restricted waterways, although a reliable and robust values must be assigned to a number of parameters when used in engineering applications.

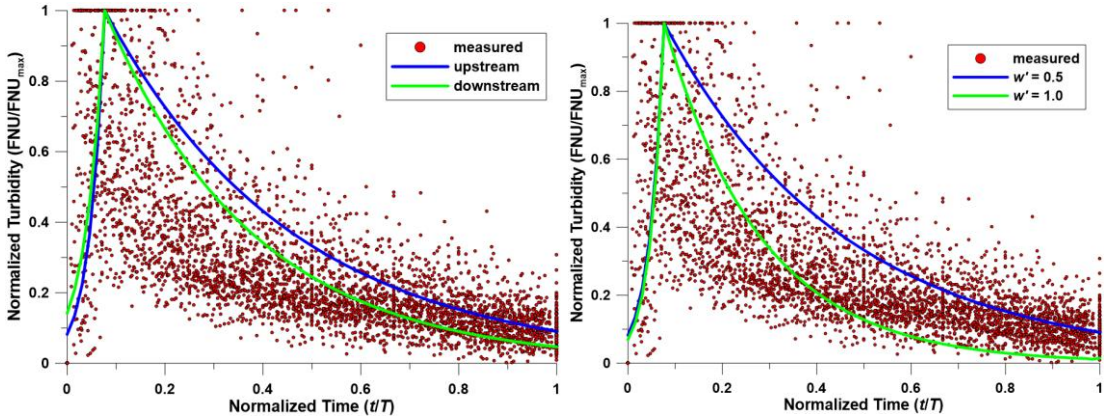

(a) (b)

Figure 8. Comparison between measured turbidity as a function of time for normalized quantities at Garn Station during 101 events and predicted turbidity for representative conditions based on the advection-diffusion equation, where (a) shows a ship with different direction of travel (upstream and downstream) and (b) includes a ship going upstream and the settling velocity varies.

6. Conclusions

The impact of ship waves, both primary (drawdown) and secondary (divergent) waves, on bed and banks in restricted waterways was studied through field data collection and different types of modeling based on empirical relationships and equations derived from simple physical descriptions. The data discussed were primarily from measurements in Göta River, which constitutes a major shipping lane on the west coast of Sweden. Both continuous recordings of turbidity at seven different stations and dedicated field campaigns during which water level and turbidity were recorded during specific ship passages were employed in the present analysis. Ship passages produced a clear signal in turbidity to which the suspended sediment concentration (SSC) was related through calibration; thus, the measurements could be used a proxy for the sediment transport.

Comparison between the measured ship waves and different predictive formulas showed that the one proposed by PIANC (1987) for secondary waves yielded the best agreement with the collected data. For the drawdown, a relationship based on the vessel sinkage (USACE, 2006) gave best results, although only a few formulas were investigated. The peak turbidity during ship passage was primarily a function of the drawdown and a simple parameterization of the generated bed shear stress due to this wave yielded satisfactory predictions in an empirical equation, although the derived coefficients are only site-specific.

A more physics-based model was developed using the advection-diffusion equation (ADE), where the ship was described as a moving source. Calibration and validation of this model with data from individual ship passages were difficult due to lack of detailed information on the ships and their properties; however, by employing representative values for the main governing parameters and normalizing the solution together

with the collected data for individual events, it was shown that the derived solution to the ADE can capture the main features of the turbidity (SSC) variation during ship passages. Before the model can be quantitatively used in engineering applications local data must be collected on ship, river, and sediment properties.

The next phase of the project will include full-scale testing of nature-based erosion protection against ship waves. The effectiveness of different nature-based solutions will be evaluated for primary and secondary ship waves as well as their ability to create hydrodynamic conditions for regenerating the fine-sediment habitats along the shores of Furusundsleden in the Stockholm Archipelago that have been lost due to the impact from ship waves.

Acknowledgements

The financial support of the Swedish Maritime Administration for parts of this study under contract No. 150950 is gratefully acknowledged. The authors would also like to thank Göteborg Vatten, who provided the turbidity data and associated information, and the hydropower company Vattenfall for the provision of flow and water level data in Göta River.

References

Abramowitz, M. and Stegun, I. 1965. *Handbook of mathematical functions*. Dover Publications Inc., New York.

Althage, J. 2010. Ship-induced waves and sediment transport in Göta River, Sweden. TVVR 10/5021, Water Resources Engineering, Lund University, Lund, Sweden.

Atzeni,A. and Sulis, A. 2012. Field measurements of tug waves in the Cagliari Harbor, Italy. *Journal of Waterway, Port, Coastal, and Ocean Engineering*, 138(1), 72-76.

Bertram, V. 2000. *Practical ship hydrodynamics.* Butterworth-Heinemann, Oxford, UK.

Carslaw, H.S. and Jaeger, J.C. 1959. *Conduction of heat in solids*. Clarendon Press, Oxford.

Crank, J. 1975. *The Mathematics of diffusion*. Clarendon Press, Oxford

Gelinas, M., Bokuniewicz, H., Rapaglia, J., and Lwiza, K.M.M. 2013. Sediment resuspension by ship wakes in the Venice Lagoon. *Journal of Coastal Research*, 29(1), 8-17.

Granath, L. 2015. ”Vågmätningar i Furusundsleden 2014. Unpublished report, Hydrografica, Stockholm, Sweden (in Swedish).

Göransson, G.I., Larson, M., Bendz, D., and Åkesson, M. 2012. Mass transport of contaminated soil released into surface water by landslides (Göta River, SW Sweden). *Hydrology and Earth System Science*, 16, 1-15.

Göransson, G., Larson, M., and Althage, J. 2014. Ship-generated waves and induced turbidity in the Göta Älv River in Sweden. *Journal of Waterway, Port, Coastal, and Ocean Engineering*, 140(3), 04014004.

Havelock, T.H. 1908. The propagation of groups of waves in dispersive media, with application to waves on water produced by a travelling disturbance. *Proceedings Royal Society of London*, Series A, 398-430.

Kriebel, D.L. and Seelig, W.N. 2005. An empirical model for ship-generated waves. *Proceeding of the 5th International Symposium on Ocean Wave Measurement and Analysis*, Madrid, Spain. (CD-ROM).

Kriebel, D.L., Seelig, W.N., and Judge, C. 2003. A unified description of ship-generated waves. *Proceedings of the PIANC Passing Vessel Workshop*, Portland, Oregon.

PIANC. 1987. Guidelines for the design and construction of flexible revetments incorporating geotextiles for inland waterways.” Working Group 4 of the Permanent Technical Committee, Permanent International Association of Navigation Congresses, Brussels.

Rapaglia, J., Zaggia, L., Ricklefs, K., Gelinas, M., and Bokuniewicz, H. 2011. Characteristics of ships’ depression waves and associated sediment resuspension in Venice Lagoon, Italy. *Journal of Marine Systems*, 85, 45-56.

Ravens, T.M. and Thomas, R.C. 2008. Ship wave-induced sedimentation of a tidal creek in Galveston Bay. *Journal of Waterway, Port, Coastal, and Ocean Engineering*, 134(1), 21-29.

Schoellhamer, D.H. 1996. Anthropogenic sediment resuspension mechanisms in a shallow microtidal estuary. *Estuarine, Coastal, and Shelf Science*, 43, 533-548.

Sorensen, R.M. 1967. Investigation of ship-generated waves. *Journal of Waterways and Harbors Division*, 93, 85-99.

Sorensen, R.M. 1997. Prediction of vessel-generated waves with reference to vessels common to the Upper Mississippi River System. ENV Report 4, U.S. Army Engineer Waterways Experiment Station, Vicksburg, MS.

Sorensen, R.M. and Weggel, J.R. 1984. Development of ship wave design information. *Proceedings of the 19th International Conference on Coastal Engineering*, ASCE, 3227-3242.

USACE 2006. Hydraulic design of deep-draft navigation projects. Engineer Manual EM 1110-2-1613, Engineering and Design, US Army Corps of Engineers, Washington DC.